Absorption of radiation by turbulent laser plasmas

V. P. Silin

P. N. Lebedev Physics Institute of the Academy of Sciences of the USSR

Usp. Fiz. Nauk **28**, 225–253 (February 1985)

A detailed review is given of modern theoretical ideas on the absorption of powerful laser radiation by plasmas. The linear theory of collisional absorption and linear wave conversion are examined, as are the results of the nonlinear theory of inverse bremsstrahlung. The results of theoretical analyses of the nonlinear interaction between radiation and moving plasmas are presented. The unusual qualitative features of the nonlinear electrodynamics of moving media that appear when the flow velocity is comparable with the velocity of sound are demonstrated. The phenomenon of field self-limitation in ultrasonic plasma flows is described. The fundamentals of the theory of parametric absorption and of the theory of absorption by plasma with well developed ion-acoustic turbulence are presented.

CONTENTS

INTRODUCTION

Physical processes governing the absorption of laser radiation have attracted attention for many years. An understanding of these processes is essential for the theoretical description of the rate at which laser energy is stored in plasma. At the same time, it is important to note that absorption by plasma in the field of powerful laser radiation is largely determined by the state of the plasma, which is then often referred to as the turbulent state. There is as yet no rigorous definition that would correspond to generally accepted ideas about plasma turbulence. However, the complexity of such absorption processes has now been established in the course of statistical and dynamic description of plasmas. At the same time, the picture of turbulent absorption that has emerged does not preclude laminar processes such as inverse bremsstrahlung and resonance absorption. We shall therefore begin with collisional absorption and linear transformation of radiation within the framework of the linear approximation (Section 1), and will then proceed to the results of the nonlinear theory of absorption by inverse bremsstrahlung (Section 2). We shall next present the dynamic theory of absorption in expanding plasmas (Section 3) and will consider separately the phenomenon of field self-limitation (Section 4) in ultrasonic plasma motion. In Section 5, we shall present results on the rate of absorption of radiation, which follow from the theory of parametric turbulence. Finally, we shall consider new results on ion-acoustic absorption (Section 6). In the concluding Section, we shall examine some experimental data on the absorption of laser radiation.

1. ABSORPTION OF RADIATION DUE TO ELECTRON-ION COLLISIONS (INVERSE BREMSSTRAHLUNG) AND RESONANCE ABSORPTION IN THE LINEAR REGIME

Collisions between plasma electrons and ions, in which the oscillation energy of electrons in the field of an electromagnetic wave is transformed into the thermal energy of electrons, constitute one of the simplest and, under certain conditions, one of the most important mechanisms governing the absorption of laser radiation by plasmas. The characteristic measure of such collisions is the electron-ion collision frequency[1] $\nu = \nu_{ei} = 4\sqrt{2\pi}e^2e_i^2n_i\Lambda \times [3(\varkappa T_e)^{3/2}m_e^{1/2}]^{-1}$ where e is the electron charge, $e_i = Z|e|$ is the ion charge, n_e is the number of electrons per cm^3, $n_i \equiv n = n_eZ^{-1}$ is the number of ions, Λ is the Coulomb logarithm ($\sim$6–20), m_e is the electron mass, and T_e is the electron temperature.

The simplest situation involving collisional absorption may be demonstrated for s-polarized radiation for which the electric vector of the electromagnetic wave is perpendicular to the direction of plasma inhomogeneity, where the plasma is assumed to be uniformly inhomogeneous. For the linear plasma profile $n_e(x) = (x/L)n_c(x \geqslant 0)$, the plasma permittivity is $\varepsilon = 1 - (x/L) + i(x/L)\nu_{ei}(x)/\omega_0$ and the critical density for which the radiation frequency ω_0 becomes comparable with the electron Langmuir frequency is $n_c = m_e\omega_0^2/4\pi e^2$. The electric field of the s-polarized electromagnetic wave satisfies the equation

$$E'' + \frac{\omega_0^2}{c^2}\left(1 - \frac{x}{L} + i\frac{\nu_e x^2}{\omega_0 L^2}\right)E = 0, \tag{1.1}$$

 0038-5670/85/020136-17$01.80

where ν_e is the electron-ion collision frequency corresponding to the critical density. Equation (1.1) refers to the case of a normally incident wave. When the characteristic linear dimensions of the plasma inhomogeneity are large in comparison with the radiation wavelength $L \gg \lambda\!\!\!^{-}_0 = c/\omega_0 = \lambda_0/2\pi$, the solution of (1.1) can be obtained in the geometric-optics approximation and takes the form

$$E(x) = \exp\left(i\int_0^x k(x)\,dx\right) + R\exp\left(-i\int_0^x k(x)\,dx\right),$$

where

$$k(x) = \frac{\omega_0}{c}\sqrt{1 - \frac{x}{L} + i\frac{\nu_c x^2}{\omega_0 L^2}}.$$

The reflection coefficient R is obtained from the condition that the electric field $E(x)$ must vanish on the critical density surface ($x = L$): $R = \exp(2i\int_0^L k(x)dx) = \exp(-i4\omega_0 L/3c)\exp(-16\nu_c L/15c)$. This expression determines the ratio of the reflected energy flux density q_R to the energy flux density q incident on the plasma: $q_R/q = |R|^2 = \exp(-32\nu_c L/15c)$. It will be useful to introduce the quantity

$$\tau = 2\int_0^L dx\,\mathrm{Im}\,k(x).$$

In our case, $\tau = (16/15)(\nu_c L/c)$. The fraction of energy absorbed by the plama is $A = 1 - (q_R/q) = 1 - \exp(-2\tau)$. Since $\nu_c = Z\Lambda\cdot 10^{11}(\lambda_0\ \mu\mathrm{m})^{-2}(T_e\ \mathrm{keV})^{-3/2}\ \mathrm{s}^{-1}$, we may write

$$A = 1 - \exp\left[-7\cdot 10^{-4}\frac{\Lambda Z(L\ \mu\mathrm{m})}{(\lambda_0\ \mu\mathrm{m})^2(T_e\ \mathrm{keV})^{3/2}}\right]. \qquad (1.2)$$

Absorption amounting to more than 10% will be assured when

$$\frac{L}{\lambda_0}Z \geqslant 10(T_e\mathrm{keV})^{3/2}(\lambda_0\ \mu\mathrm{m}). \qquad (1.3)$$

Hence it is clear that inverse bremsstrahlung will be ineffective when (a) L is small, which occurs for short laser pulses, (b) the plasma has a high enough effective ion charge Z, (c) the electron temperature T_e is high enough, and (d) the laser wavelength is long enough, e.g., in the case of CO_2-lasers. Conversely, (1.1) is more readily satisfied for short-wavelength laser radiation. For example, for $\lambda_0 = 0.35\ \mu$m, this condition assumes the form $(L\ \mu\mathrm{m})Z \gtrsim (T_e\ \mathrm{keV})^{3/2}$.

Additional analysis is necessary when the laser radiation has a p-component, i.e., when the radiation is polarized so that the electric vector of the wave has a non-zero component in the direction of the spatial inhomogeneity of the plasma. This component gives rise to electron motion in the direction of the inhomogeneity, which produces charge separation and small plasma oscillations in the region of the critical-density layer in which the electron oscillations in the laser wave field are in resonance with electron Langmuir oscillations.

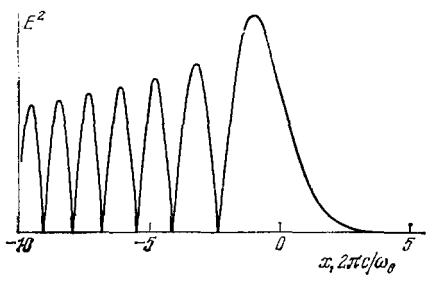

FIG. 1. Electric field in an s-polarized wave as a function of position in an inhomogeneous laser plasma.

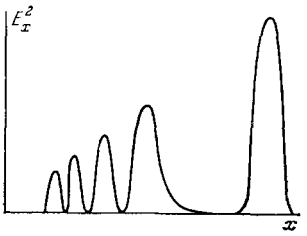

FIG. 2. Field in a p-polarized wave as a function of position.

Figure 1 shows the spatial distribution of the electric field in s-polarized radiation in plasma when the radiation intensity increases in the direction of the inward normal to the plasma surface. It reaches the critical density at normal incidence, and is reflected from the layer of density $n_c\cos^2\theta$ where θ is the angle of incidence. As the point of reflection $x/L = \cos^2\theta$ is approached from the lower-density side, the characteristic scale of the spatial variation of the field increases from the vacuum wavelength $\lambda\!\!\!^{-}_0 = \lambda_0/2\pi = c/\omega_0$ to $\lambda\!\!\!^{-}_0(L/\lambda\!\!\!^{-}_0)^{1/3}$. This growth in the spatial scale of the field is accompanied by an increase in its amplitude, which is governed by the factor $(L/\lambda\!\!\!^{-}_0)^{1/3}$. To the right of the point of reflection, the electromagnetic field falls off exponentially over the distance $\sim\lambda\!\!\!^{-}_0(\sin\theta)^{-1}$. The p-polarized wave (Fig. 2) can reach the critical-density layer on which plasma resonance occurs ($\omega_0 = \omega_{Le}$), i.e., it can penetrate the plasma to a distance $\sim L\sin^2\theta$ if the condition for optimum angle of incidence, i.e., $\sin\theta_{opt} \sim (\lambda\!\!\!^{-}_0/L)^{1/3}$, is satisfied. A detailed theory of the propagation of s-polarized waves under the conditions of plasma resonance has been constructed by Denisov[3] (see also Refs. 2 and 4). However, Denisov[3] did not determine the rate of absorption of electromagnetic radiation near resonance. The rigorous set of equations that takes into account the longitudinal wave-field component in the neighborhood of resonance was formulated in a paper by Piliya.[5] However, Omel'chenko and Stepanov[6] have shown that the conclusions reported in that paper in relation to the rate of absorption are inaccurate. We note that, in his book,[7] Budden points out the strong absorption in the neighborhood of plasma resonance with p-polarized electromagnetic radiation. Numerical solution of the field equations[8,9] has confirmed strong (resonant) absorption of up to 50% in the neighborhood of the plasma resonance. A self-consistent analytic theory of resonant absorption has also been developed,[10,11] with the theory of Ref. 6 as its limiting case for small angles of incidence. In particular, it was shown that Denisov's theory[3] of the electromagnetic field in the neighborhood of plasma resonance was in qualitative agreement with the behavior of resonant absorption, except that it overestimated maximum absorption by a factor of 1.4.

We shall now use Denisov's approach[3] as a basis for a

theory of resonant absorption when wave dissipation is determined by the collision frequency ν_c. Accordingly, the longitudinal electric-field component E_x near the resonance point $x = L$ will be related to the magnetic field B_z as follows:

$$\varepsilon E_x \equiv \left(1 - \frac{x}{L} + i\frac{\nu_c}{\omega_0}\right) E_x(x) = B_z(L)\sin\theta. \qquad (1.4)$$

In its turn, the magnetic field in the neighborhood of resonance will be related to the amplitude B of the magnetic field incident on the plasma from vacuum by the following expression:

$$\sin\theta\, B_z(L) = \left(\frac{\lambda_0\cos\theta}{2\pi L}\right)^{1/2} \tilde{\Phi}\left(\left(\frac{L}{\lambda_0}\right)^{1/3}\sin\theta\right) B, \quad (1.5)$$

where[3] $\tilde{\Phi}(\tau) = 4\tau\sqrt{\pi}\,[\mathrm{Ai}^3(\tau^2)/\dot{\mathrm{A}}\mathrm{i}(\tau_2)]^{1/2}$ and Ai and Ȧi are the Airy function and its derivative, respectively. A graph of the function $\tilde{\Phi}$ is shown in Fig. 3.

The power absorbed by the plasma is largely determined by the work done by the component E_x. Assuming that $\nu_c \ll \omega_0$, we have $Q = (cB^2\cos\theta/8\pi)\tilde{\Phi}^2((L/\lambda_0)^{1/3}\sin\theta)$. The ratio of the last expression to the energy flux density incident on the plasma $q = (cE^2\cos\theta/4\pi) = (cB^2\cos\theta/4\pi)$ is the absorption coefficient $A = (1/2)\tilde{\Phi}^2((L/\lambda_0)^{1/3}\sin\theta)$. In view of Pert's result,[11] we can now write down the following interpolation formula:

$$A = 18\sin^2\theta\left(\frac{L}{\lambda_0}\right)^{2/3}\left|\frac{\mathrm{Ai}^3((L/\lambda_0)^{2/3}\sin^2\theta)}{\mathrm{Ai}\,((L/\lambda_0)^{2/3}\sin^2\theta)}\right|, \qquad (1.6)$$

which differs from the previous expression by a numerical factor. At optimum incidence, this expression yields values of up to about 50%. We recall at this juncture that the absorption process that we have examined is due to electron-ion collisions. On the other hand, the fact that (1.6) does not contain the collision frequency is due to the resonant increase in the electric field in the neighborhood of the critical plasma density. We emphasize that resonant absorption will also occur when the field energy flux from the region of plasma resonance is determined by longitudinal electron Langmuir oscillations excited in this region. The field of such waves is described by the following equation when collisions are neglected:

$$\left(1 - \frac{x}{L}\right) E_x + 3r_{De}^2\frac{d^2E_x}{dx^2} = B_z(L)\sin\theta, \qquad (1.7)$$

where r_e is the electron Debye length. The characteristic distance for a change in the electric field E_x is then $(\delta x)_l \sim (Lr_{De}^2)^{1/3}$ whereas, according to (1.3), the corresponding expression for the situation dominated by collisions is $(\delta x)_{st} \sim (\nu_c/\omega_0)L$. Comparison of these two expressions shows that the collision mechanism becomes unimportant when $\nu_c/\omega_0 < (r_{De}/L)^{2/3}$. The electromagnetic radiation is then transformed in the region of resonance into longitudinal plasma waves, with the transformation coefficient given by an expression identical with (1.6). Since plasma waves generated by this transformation are subsequently absorbed by plasma electrons, this coefficient is also the coefficient of absorption of electromagnetic radiation. However, we must emphasize at this point that the absorption of plasma waves may be due to a number of different mechanisms. Absorption due to electron-ion collisions leads to an increase in the temperature of the main mass of electrons. Another absorption mechanism involves collisionless Landau damping in which the plasma wave is absorbed as a result of Cherenkov interactions with electrons. According to (1.7), the plasma wave field falls exponentially toward the dense plasma region $x > L$, but the wave *can* propagate in the direction of the lower-density region $0 < L < x$. However, the same equation (1.7) predicts that the wave vector of the plasma wave increases with distance from the resonance region in accordance with the expression $k_x(x) = r_{De}^{-1}\sqrt{(L-x)/3L}$. When $k_x r_{De}$ reaches about 0.2 under these conditions, the Landau damping, ignored in (1.7), leads to the almost complete absorption of plasma waves. This type of collisionless absorption results in the generation of fast (suprathermal) electrons.

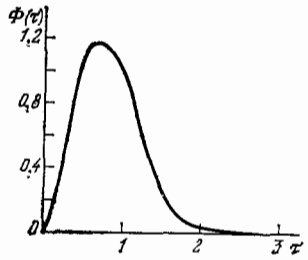

FIG. 3. The Denisov function.

The simple model, in which plasma is inhomogeneous in one direction only, leads to substantial absorption only when the angle of incidence has the optimum value given by $\sin\theta_{opt} \sim (\lambda_0/L)^{1/3}$. Resonant absorption is more readily attained in two-dimensionally, and also in three-dimensionally, inhomogeneous plasma. When, for example, the plasma density is a wavelike function of position along the y axis, the angle of incidence assumes the optimum value in a number of segments lying along this axis. This is particularly important when the characteristic inhomogeneity scale along the y axis is close to the wavelength of the electromagnetic field. Figure 4 shows the dependence on the angle of incidence obtained in Ref. 12 for the absorption coefficient of plasma in which the density inhomogeneity is described by $n_e(x, y) = n_c(x + \mu\sin ky)L^{-1}$. The broken line corresponds to the usual dependence given by (1.6), and curves 1 and 2 represent $\mu k(L/\lambda_0)^{1/3} = 0.6$ and 0.4.

Even more favorable for resonant absorption is the

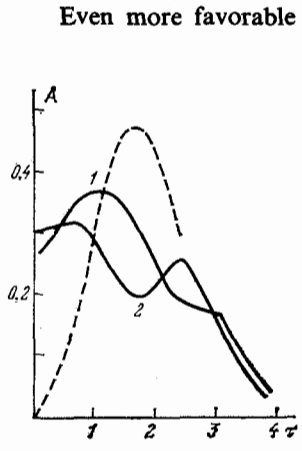

FIG. 4. Absorption in a plasma with a corrugated density distribution.

presence of a magnetic field which can give rise to almost 100% absorption of the extraordinary wave by the plasma.[12-14] It is important to emphasize, however, that almost 100% resonant absorption is also possible in the absence of a magnetic field when a more complicated dependence of density on position ensures better matching between the incident electromagnetic wave field and the absorbing load, i.e., the plasma.[15,16] This means that the magnitude of resonant absorption by a real plasma-density profile may exceed the value predicted by (1.6). We shall see later, when we consider the dynamic variation in the density profile of an expanding plasma, that resonant absorption is determined by plasma density dynamics.

Spatial inhomogeneity of plasma density and temperature distributions, unaccompanied by an inordinate reduction in the spatial inhomogeneity scale, does not produce a qualitative change in the optical thickness or absorption coefficient at normal incidence of the wave on the plasma, since these are determined by electron-ion collisions. However, the angular dependence of absorption depends in an important way on the form of the density and temperature as functions of the coordinates.[17] In the special case $T_e = \text{const}$, $n_e \sim x$ that corresponds to Eq. (1.1), it turns out that $\tau(\theta) \sim \cos^5\theta$. Next, the law $\tau(\theta) \sim \cos^3\theta$ is valid for both $T_e = \text{const}$ and $n_e = \exp(-x/x_0)$ and $n_e \sim x$ and $n_e T_e^{-3/2} = \text{const}$. Finally, $\tau(\theta) \sim \cos\theta$ when $n_e T_n^{-3/2} = \text{const}$ and $n_e \sim x$. The corresponding three curves are shown in Fig. 5 in which it is assumed that the absorption coefficient is 30% at normal incidence.

2. ABSORPTION BY INVERSE BREMSSTRAHLUNG—THE NONLINEAR REGIME

Inverse bremsstrahlung is a nonlinear process that has for long attracted the attention of researchers. It occurs when the amplitude of electron velocity oscillations, $v_E = |e|E/m\omega_0$, in the electromagnetic wave field exceeds the thermal electron velocity $v_{Te} = \sqrt{\varkappa T_e/m_e}$. Since the effective collision frequency is inversely proportional to the cube of the electron velocity, we have the corresponding nonlinear dependence on the field in the effective electron-ion collision frequency, which determines dissipation due to the inverse bremsstrahlung effect. Apart from this nonlinear effect, there is also the logarithmic dependence due to the variation in the minimum impact parameter under the influence of the electric field and, for plane-polarized radiation, the fact that the electron oscillation velocity increases slightly in each oscillation period. This combination of effects was examined in Ref. 18 on the basis of the classical transport equations for fast plasma processes in strong fields[19,20] (see also Ref. 1). The publication of Ref. 18 was followed by a number of papers on nonlinear inverse-bremsstrahlung absorption, aimed at the development of a quantum theory (see Ref. 21, and the references therein, for a critical review of the subject).

The heat liberated per unit plasma volume as a result of inverse bremsstrahlung is given by

$$Q_\alpha = n_e m_e v_E^2 \nu_\alpha(E), \tag{2.1}$$

where the nonlinear effective electron collision frequency, which depends on the polarization α, can be written as[21]

$$\nu_\alpha(E) = \frac{8e^2e_i^2n_i}{m_e^2v_E^3} R_\alpha(E). \tag{2.2}$$

In the simple case of circular polarization, the minimum impact parameter for which we can use perturbation theory for the electron-ion interaction problem is $r_s = 4Ze^2/m_e v_E^2$. We now assume a Maxwellian velocity distribution, and also that the amplitude of the electron oscillation velocity is much greater than the thermal velocity ($\varkappa T_e \gg \hbar\omega_0$). Moreover, the distance $v_{Te}\omega_0$ traversed by a thermal electron in one field period is assumed large in comparison with the minimum impact parameter r_s which in turn is large in comparison with the de Broglie wavelength. We then have

$$R_s = \frac{\pi}{\sqrt{2}} \ln\frac{v_{Te}}{\omega_0 r_s}. \tag{2.3}$$

This and many other formulas were obtained in Refs. 21–23, and practically exhaust all possible relationships between $\varkappa T_e$ and $\hbar\omega_0$, and also between the de Broglie wavelength and minimum impact parameter.

For plane polarized radiation, the characteristic relations are those containing products of logarithms. We shall now produce the simple formula corresponding to the classical limit $Ze^2 \gg \hbar v_E$ for which the distance v_{Te}/ω_0 traversed by a thermal electron in one field period is large in comparison with $Ze^2/\varkappa T_e$. For plane-polarized radiation we then have

$$R_l = \left(\ln\frac{v_E}{v_{Te}}\right) \ln\frac{\varkappa T_e v_E}{Ze^2\omega_{Le}}. \tag{2.4}$$

The factor $\ln(v_E/v_{Te})$ in this expression is due to the fact that the electron oscillation velocity vanishes periodically in the plane wave. Quantum-mechanical effects in electron-ion collisions in the field of a strong plane-polarized electromagnetic wave were taken into account in Ref. 21.

According to Ref. 24, another nonlinear reduction in inverse-bremsstrahlung absorption is due to the modification by the field of the symmetric part of the electron distribution, which becomes increasingly non-Maxwellian with increasing ion charge and energy of electron oscillations in the field of the electromagnetic wave. As a result, the electron distribution approaches the function $\exp(-v^5/v_0^5)$. A detailed theory of the distribution of electrons in strong electromagnetic fields is given in Ref. 25. According to Ref. 26, the qualitative reduction in the optical thickness, due to this

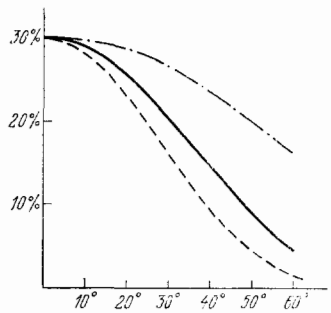

FIG. 5. Angular dependence of the optical thickness of plasma.

modification of the electron distribution, is described by the factor

$$1-0.533\left\{1+\left[\frac{0.27}{Z}\left(\frac{m_e\omega_{Le}v_{Te}}{eE_0}\right)^2\right]^{0.75}\right\}^{-1}. \quad (2.5)$$

It follows from this that the optical thickness can decrease by a factor of two for values of Z that are not small.

We note that, apart from the above reduction in inverse-bremsstrahlung absorption effects, absorption is also substantially reduced by the steepening of the plasma density profile under the influence of the ponderomotive force produced by the powerful radiation.

3. ABSORPTION OF RADIATION BY NONSTATIONARY MOVING PLASMA

When powerful electromagnetic radiation acts on plasma expanding into a vacuum, the field energy is transferred to the plasma not only through collisions and resonant transformation, but also by ponderomotive forces. These forces are due to both the incident radiation and the longitudinal waves generated in course of resonant transformation. The effect of p-polarized radiation on plasmas is of particular interest in this connection. Below, we present some of the results obtained in the dynamic approach to this phenomenon, based on the researches of Andreev, Silin, and Stenchikov[28–33] who examined the self-consistent dynamic picture in plasma electrodynamics and hydrodynamics, augmented by electron kinetics. This enables us to see the entire range of the associated phenomena.

We shall model the dynamic interaction between radiation and plasma by considering a plane-parallel layer of fully ionized plasma with ion density $n(x, t)$ increasing in the direction of the x axis. We shall suppose that the following electromagnetic field is incident from the region $x<0$ at an angle θ to the density gradient:

$$\mathbf{k}_0=\frac{\omega_0}{c}\{\cos\theta,\ \sin\theta,\ 0\},\quad \mathbf{B}_0=\{0,\ 0,\ B\},$$

$$\mathbf{E}_0=\{E_x,\ E_y,\ 0\},\quad \mathbf{B}=\mathbf{B}(x,\ t)\exp\left\{-i\omega_0\left[t-\frac{y}{c}\sin\theta\right]\right\},$$

$$\mathbf{E}_0=\mathbf{E}(x,\ t)\exp\left\{-i\omega_0\left[t-\frac{y}{c}\sin\theta\right]\right\}, \quad (3.1)$$

where ω_0 is the field frequency and $\mathbf{B}$ and $\mathbf{E}$ are the magnetic and electric fields, respectively. We shall use for the electric field the usual truncated equations that take into account nonlinear effects through the permittivity $\varepsilon=1-(zn/n_c)[1-i(\nu_e/\omega_0)]$ which contains the ion density $n(x, t)$ that is a nonlinear function of the field. The damping of the longitudinal field component is characterized in these equations by the Landau damping that is a functional of the electron distribution function which, in turn, is a solution of the quasilinear equation.

Next, the ion density and, with it, the permittivity, will vary because of plasma dynamics described by the hydrodynamic equations

$$\frac{\partial n}{\partial t}+\frac{\partial(nv)}{\partial x}=0,$$
$$\frac{\partial(nv)}{\partial t}+\frac{\partial}{\partial x}[n(v^2+v_s^2)]+\frac{Ze^2n}{4M_1m_e\omega_0^2}\frac{\partial|\mathbf{E}|^2}{\partial x}=0, \quad (3.2)$$

which include the ponderomotive force. Here, $v_s^2=\varkappa(ZT_e+3T_i)/M_i$ is the square of the ion sound velocity and Z and M_i are, respectively, the ion charge and mass. We shall use (3.2) with the assumption of a spatially uniform electron temperature distribution, which corresponds to the assumption that the electron mean free path λ_{Te} is much greater than the linear dimensions of the region in which most of the field energy is liberated in the plasma.

The field equation for the fundamental frequency ω_0 of the radiation enables us to determine the nonlinear current at frequency $N\omega_0$, which is responsible for the excitation of the Nth harmonic of the electromagnetic field in the plasma. For our plane-parallel layered medium, the Nth harmonic may be characterized by the z-component of the magnetic field

$$\mathbf{B}_{N\omega_0}(x,\ y,\ t)=\left\{0,\ 0,\ B_N(x,\ t)\times\exp\left[-iN\omega_0\left(t-\frac{y}{c}\sin\theta\right)\right]\right\}, \quad (3.3)$$

for which the field equation is determined by the nonlinear current $\mathbf{j}^{(N)}$. In particular, for the second harmonic, we have

$$\mathbf{j}^{(2)}=\frac{ie}{8\pi\omega_0m_e}\left(\mathbf{E}_0\,\mathrm{div}\,\mathbf{E}_0+\frac{\omega_{Le}^2}{4\omega_0^2}\,\mathrm{grad}\,|\mathbf{E}_0|^2\right), \quad (3.4)$$

where $\mathbf{E}_0=(E_x, E_y, 0)$ is the solution of the truncated equations for the field at fundamental frequency.

We emphasize that the field equation for the harmonics must be augmented by boundary conditions describing free emission of radiation into the vacuum and wave reflection from the dense-plasma region ($n>4n_c$ in the case of the second harmonic). The resulting solution determines the energy transformation coefficient for the incident radiation. For example, for the second harmonic, this becomes

$$K_2=\left(\frac{B_2}{B_0}\right)^2,$$

where B_2 and B_0 are the magnetic field of the second harmonic and of the incident radiation in vacuum, respectively.

A numerical solution of the set of field equations and nonlinear hydrodynamic equations is described in Ref. 30. The equations were solved numerically for the region $0\leqslant x\leqslant L$ of length equal to a few vacuum wavelengths ($L\geqslant 30\lambda_0$) and containing the point $Zn=n_c$. The initial densities $n(x, 0)=n_0(x)$ and velocities $u(x, 0)=u_0$ were specified at the time $t=0$, and the stationary solution on the density profile n_0 was taken as the initial electromagnetic field. The turning-on of the radiation incident on the plasma was simulated by a linear rise in incident-wave energy, followed by constant illumination (Fig. 6).

We must now consider boundary conditions for the hydrodynamic variables, which depend on the plasma velocity at $x=0$ and $x=L$. For ultrasonic plasma influx velocities in the region of interaction with radiation $u(L, t)<-v_s$, the density and velocity were specified at $x=L$: $n(L, t)=n_0(L)$, $u(L, t)=u_0(L)$. For subsonic influx velocities $|u(L, t)|<v_s$, only one boundary condition, either for density or velocity, need be specified at $x=L$. The left-hand boundary at $x=0$ was assumed to be free for the ultrasonic plasma influx $u(0, t)<-v_s$ whereas, for subsonic flow, it was simulated by taking the plasma density in the form $n(0, t)=n_0(0)$.

The electron distribution function was determined only

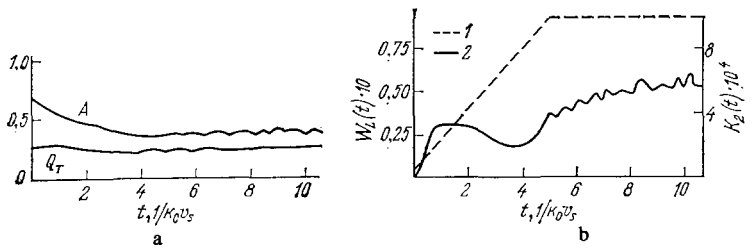

FIG. 6. Ultrasonic expansion: a—time dependence of absorption coefficient A and fraction Q_T of absorbed energy due to collisions; b—laser pulse shape $W_L(t)$ (curve 1) and time dependence of the coefficient of transformation of radiation into the second harmonic (curve 2).

in the region of localization of Langmuir oscillations ($x_l < x < x_l + l_d$), using the boundary condition corresponding to the entry of electrons into this region with the Maxwellian distribution and temperature equal to the plasma temperature near the critical-density layer. The accelerated electrons leave the region of quasilinear diffusion freely. However, on the boundary with vacuum, fast electrons reenter the plasma, and this symmetrizes the electron velocity distribution. We emphasize that both the hydrodynamic and electrodynamic nonlinearities lead to the transfer of energy to small-scale perturbation modes. Short-wave perturbations are efficiently absorbed by electrons as a result of the Cherenkov interaction. This produces a substantial smoothing of the solutions, and restricts the spectrum to wavelengths that are admissible by Landau damping.

Two types of initial condition were used to obtain the solutions of the set of hydrodyamic, kinetic, and electrodynamic equations. In the first case, the flow was characterized by comparable magnitudes of plasma velocity and density gradients whereas, in the second case, the corresponding scales could differ substantially from each other.

The solution of the set of equations of electrodynamics, hydrodynamics, and kinetics was implemented by program LAST[30] (Light Absorption by Strong Turbulence).

Let us begin by considering the results for comparable velocity and density gradients in the initial conditions, for which the initial state ($t = 0$) can be described by the rarefaction wave $n(x) = n_c \exp[(x - x_c)/l]$, $u(x) = -v_c + v_s(x - x_c)/l$ (v_c is the absolute magnitude of the plasma velocity at the critical-density point x_c and l is the characteristic spatial scale of density and velocity changes: $l = v_s t_0$, where t_0 is the time at which the rarefaction wave is produced), which is an exact solution of the equations of isothermal hydrodynamics, with the ponderomotive force neglected, which can be justified for the initial phase of interaction with the rising radiation pulse.

Numerical integration under initial rarefaction-wave conditions was performed for the following parameter values that were close to those used in the experiment: $T_{e0} = 1.25$ keV, $v_E/c = 0.015$, where $v_E = |e|E_{inc}/m_e\omega_0$ is the amplitude of the electron population velocity in the field of the pump wave in vacuum. For the neodymium-glass laser ($\omega_0 = 1.8\cdot 10^{15}\ s^{-1}$), the latter corresponds to the energy flux density $q = 5\times 10^{24}$ W/cm^2. The initial inhomogeneity scale was assumed to be $l = 10\lambda_0$ and corresponded to the ultrasonic plasma flow with a sharp density and velocity gradient. The angle of incidence was taken to be $\theta \approx 17°$($\sin\theta = 0.29$), and the effective collision frequency was specified by the ratio $\nu_c/\omega_0 = 5\cdot 10^{-3}$.

Figure 6 shows the time-dependence of the absorption coefficient A, the fraction of energy absorbed as a result of collisions Q_T, and the shape of the laser pulse $W_L(t) = E_{inc}^2(t)/4\pi n_c \varkappa T_{e0}$. The reflection coefficient $R(t)$ for laser radiation (at $x = 0$) determines the absorption coefficient through the expression $A = 1 - |R(t)|^2$. The fraction Q_T of energy absorbed as a result of collisions, and expended in heating most of the plasma electrons, is given by

$$Q_T \frac{c}{8\pi} |E_0|^2 \cos\theta = \int_0^L dx \nu_c \frac{n}{n_c} |E(x, t)|^2.$$

Figure 6b also shows the time dependence of the coefficient of transformation of incident radiation into the second harmonic. Figure 6 shows that, initially, there is a reduction in absorption and a relatively large difference between A and Q_T. This is due to the rise in the internal longitudinal field in the plasma when the radiation is turned on. Next, the coeffi-

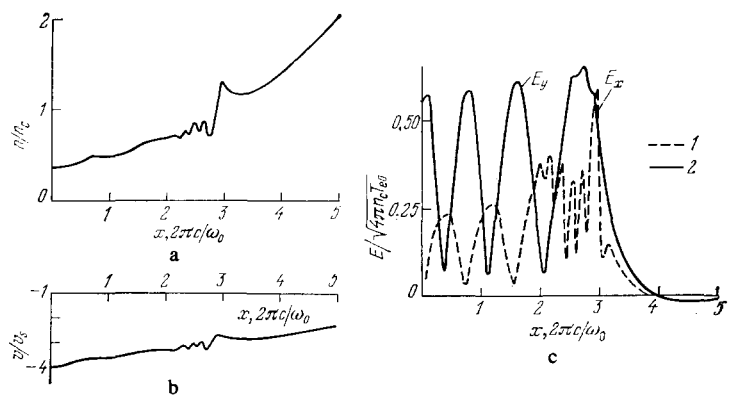

FIG. 7. Plasma density (a), plasma velocity (b), and electric field (c) as functions of position (1—E_x, 2—E_y; ultrasonic plasma expansion).

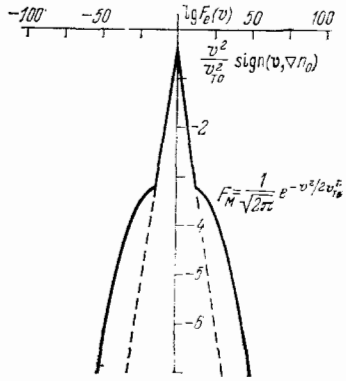

FIG. 8. Distribution of electrons accelerated by the Cherenkov mechanism in the case of ultrasonic expansion of plasma.

cient of transformation into the second harmonic rapidly ceases to be proportional to $W_L(t)$. This is due to the fact that, for $t \sim (k_0 v_s)^{-1}$, the plasma density profile begins to deform in the neighborhood of the critical density. In particular, a sharp jump is formed at the critical density point. A quasistationary regime occurs for times $t \gtrsim 7(k_0 v_s)$. It is characterized by the relationships shown in Fig. 7 and corresponds to $t = 8(k_0 v_s)^{-1}$. The absorption coefficient is $A \simeq 40\%$ and the fraction of energy expended in the collisional heating of the main mass of electrons is about 25%, whereas 15% of the incident radiation energy is transferred to "fast" electrons as a result of Cherenkov interactions. The electron distribution is then of the form shown in Fig. 8, where reflection of fast electrons from the plasma boundary is taken into account. It is clear that hot electrons appear within a small velocity interval.

A qualitatively different picture may arise when the characteristic scale l of the initial velocity distribution is varied. To simulate this, we have carried out a numerical calculation with the initial conditions

$$n(x, 0) = n_c \left(1 + \frac{x - x_c}{l_n}\right), \quad u(x, 0) = -v_c \left(1 + \frac{x - x_c}{l_n}\right)^{-1}, \tag{3.5}$$

which correspond to the uniform flux $n(x, 0)u(x,0) = -n_c v_c$ with a linear density profile. In a small neighborhood of the critical density point, the initial conditions (3.5) lead to a formula for the form of the rarefaction wave with characteristic spatial scale $l = (v_s/v_c) l_n$. The inhomogeneity scale then depends on the velocity at the critical point ($n = n_c$). Our calculations have shown that this dependence is very important. In particular, for ultrasonic values of v_c, the characteristic scale of the spatial variation is relatively small, and the initial conditions (3.16) and (3.17) lead to a picture that is in many respects similar to Figs. 6–8. A different situation arises for small values of v_c.

Figures 9–11 show numerical solutions of (3.2)–(3.8) with initial conditions $v_c = 0$ (all the other parameters are the same as in Figs. 6–8).

Comparison of Figs. 6 and 9, which characterize the dynamics of absorption at the fundamental frequency, and of emission at the second harmonic frequency $2\omega_0$, demonstrates a qualitative difference. Thus, we have sharp absorption peaks of up to 100% *and* a considerable (by more than an order of magnitude) increase in the transformation of radiation into the second harmonic. The latter is a particularly important indication of the considerable increase in the electromagnetic field in the plasma. The correlation between harmonic generation and absorption peaks indicates that the internal field plays an important role in the radiation energy transfer to plasma. Figure 10 demonstrates the spatial distribution of velocity and density, and of the electromagnetic field for $t = 11.5/(k_0 v_s)$. It is important to emphasize the presence of cavitons, i.e., regions of space bounded by "humps" with postcritical densities ($n > n_c$), which trap and amplify the field of longitudinal Langmuir oscillations. It is precisely at such instants of formation of cavitons and of field trapping that absorption becomes particularly high ($A \simeq 95\%$), and more than half the absorbed energy is expended in generating "hot"electrons ($Q_F \simeq 40\%$). We emphasize once again the dynamic character of harmonic generation and absorption, which is due to the appearance and annihilation of cavitons. While this is happening, the plasma can assume states that reflect larger amounts of energy than are incident upon the plasma at that time. This is due to the reflection of field energy stored in cavitons.

Figure 11 shows the electron distribution function for $t = 11.5/(k_0 v_s)$, which is qualitatively different from the distribution of Fig. 8, obtained for ultrasonic expansion. We note that the presence of cavitons trapping the Langmuir wave energy leads to an effective acceleration of electrons in both directions. Further, $T_{hot} \approx 7T_{e0}$, and this distribution obtains in a wide velocity interval, which corresponds to a wide spectrum of Langmuir oscillation wavelengths in the interior of the cavitons.

Calculations with small but finite value of v_c and initial condition (3.5) preserve the caviton picture, which vanishes only for large v_c. Thus, for $|u(L, t)| = 0.5 v_s$ when $l_n = 41\lambda_0$ and $l = 49\lambda_0$), i.e., for relatively small inhomogeneity scales, there is an increase in the number of cavitons, and the pro-

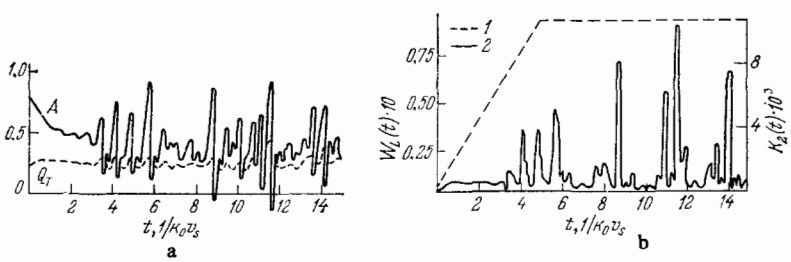

FIG. 9. Subsonic expansion: a—time dependence of the absorption coefficient and fraction Q_T of collisionally absorbed energy; b—laser pulse shape (1) and time dependence of the coefficient of transformation of energy into the second harmonic (2).

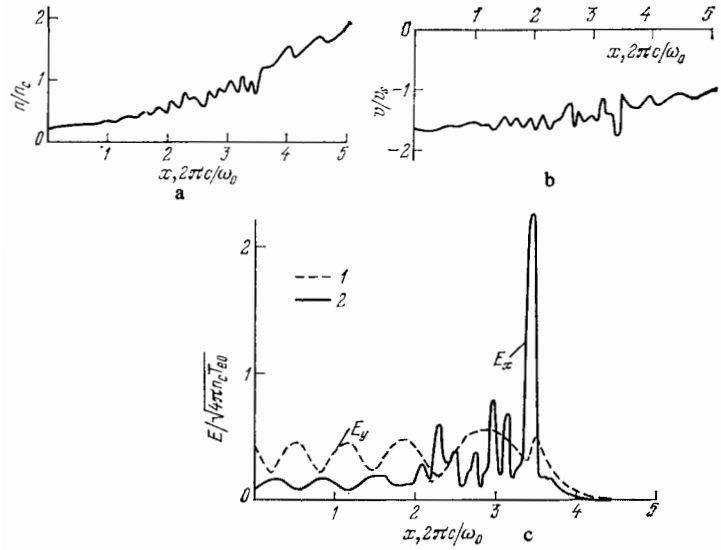

FIG. 10. Plasma density (a), plasma velocity (b), and electric field (c) as functions of position (1—E_y, 2—E_x; subsonic plasma expansion).

cess whereby they are formed becomes quasistationary. Figure 12 shows the temporal evolution of the plasma density distribution, characterized by the caviton structure, and Fig. 13 shows the time dependence of the absorption coefficient that corresponds to this structure.

Summarizing our dynamic analysis of absorption of powerful radiation by plasmas, we may conclude that there is a number of different regimes of interaction between radiation and plasmas. Thus, on the one hand, when the velocity gradient is relatively smooth, we have the caviton regime in which cavitons are filled with a strong and short-wave field that produces an effective transfer of energy to hot electrons. In the opposite situation, in which there is a steep velocity gradient, we have established the conditions under which caviton formation is impeded, and we find that the internal fields in the plasma, as well as harmonic generation and the generation of hot electrons, are suppressed. We may therefore suppose that, when powerful radiation interacts with plasmas, the turbulent states that arise in the latter may assume diametrically different forms.

We note that combined calculations of local field structure and plasma flow in the region of absorption, using the program LAST, and of global hydrodynamic expansion, using the program MEDUSA, have demonstrated the importance of the regimes examined above.[34]

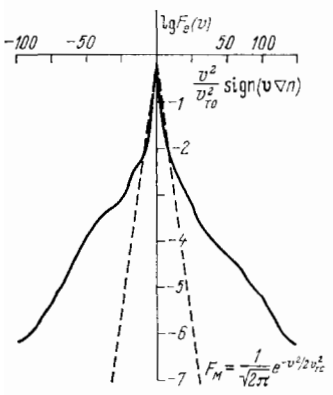

FIG. 11. Distribution of electrons acclerated by the Cherenkov mechanism in subsonic plasma expansion.

4. FIELD SELF-LIMITATION EFFECT

It was shown in the last section that the change in the spatial density distribution and plasma velocity produced by ponderomotive forces has a qualitative effect on relationships describing the absorption of radiation. We shall now examine, in this context, some of the consequences of the nonlinear electrodynamics of ultrasonic plasma flow, including some propositions that have been established analytically. In particular, we shall examine the consequences of nondissipative time-independent one-dimensional plasma hydrodynamics based on the equations

$$\frac{\partial (nu)}{\partial x} = 0, \quad u\frac{\partial u}{\partial x} = -\frac{1}{n}\frac{\partial n v_s^2}{\partial x} - \frac{Ze^2}{4m_e M_1 \omega_0^2}\frac{\partial |\mathbf{E}|^2}{\partial x}. \quad (4.1)$$

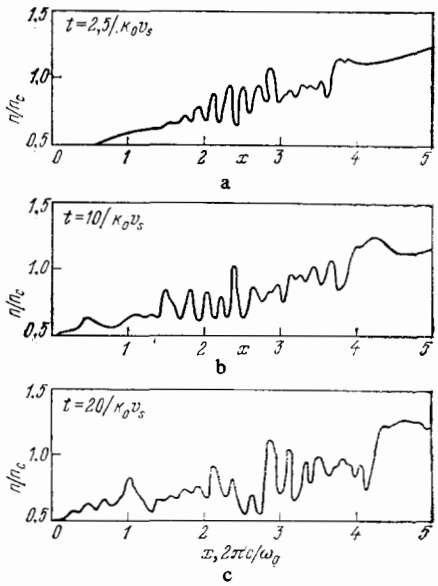

FIG. 12. Temporal evolution of plasma density.

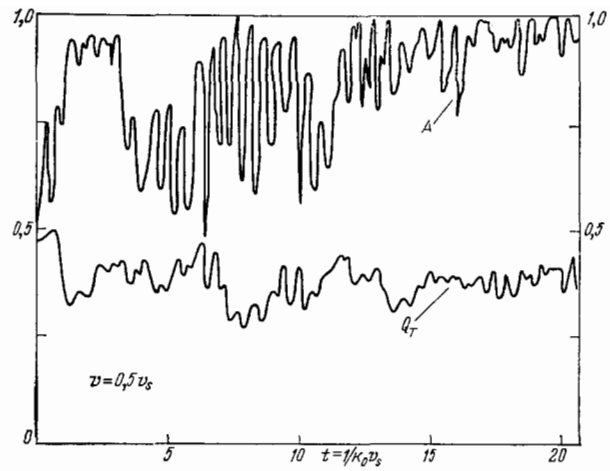

FIG. 13. Temporal evolution of absorption coefficient A and fraction Q_T of collisionally absorbed energy.

This set of equations has the following two integrals: $(1/2)u^2(x) + v_s^2 \ln n(x) + Ze^2|\mathbf{E}(x)|^2(4m_e M_i \omega_0^2)^{-1} = (1/2)V^2 + v_s^2 \ln N = \text{const}$, $n(x)u(x) = NV = \text{const}$.

These formulas enable us to write down one equation for the relation between the plasma ion density and the electric field amplitude, namely,

$$\frac{1}{2}V^2\left(1-\frac{N^2}{n^2(x)}\right)+v_s^2\ln\frac{N}{n(x)}=\frac{Ze^2\,|\,\mathbf{E}(x)\,|^2}{4m_eM_i\omega_0^2}. \tag{4.2}$$

With the permittivity given by

$$\varepsilon(\omega,\ |\mathbf{E}(x)|^2)=1-\frac{Zn(x)}{n_c}\ , \tag{4.3}$$

this expression is the constitutive relation that leads to different electrodynamic consequences for subsonic and ultrasonic time-independent plasma flows. On the other hand, the differences can also be seen qualitatively by examining the following equation that ensues from (4.1):

$$(u^2-v_s^2)\frac{1}{n}\frac{\partial n}{\partial x}=\frac{Ze^2}{4m_eM_i\omega_0^2}\frac{\partial\,|\,\mathbf{E}(x)\,|^2}{\partial x}.$$

This shows that, in a subsonic flow ($u^2 < V_s^2$), the maximum electric field strength corresponds to minimum plasma density, which leads to the nonlinear focusing of the field in the plasma. Contrariwise, equation (4.6) shows for the ultrasonic flow that the ponderomotive force rakes up the plasma into the strong-field region. Theoretical indications of the latter possibility can be found in the literature.[35–37] Direct experimental confirmation of this plasma behavior was reported in Ref. 38.

To demonstrate the unusual electrodynamics of ultrasonic plasma flow, let us consider the simple consequences that readily follow for the weakly nonlinear state in which the electromagnetic field pressure is small in comparison with thermal pressure. We may then assume that $n(x) = N + \delta n(x)$, $u(x) = V + \delta u(x)$ in (4.2), where δn and δu are small, so that

$$\delta n=\frac{NZ\,|\,\mathbf{E}(x)\,|^2}{(V^2-v_s^2)\,16\pi n_c M_i},\quad \delta u=-\frac{VZ\,|\,\mathbf{E}(x)\,|^2}{(V^2-v_s^2)\,16\pi n_c M_i}. \tag{4.4}$$

According to (4.3), these expressions enable us to write the permittivity in the form

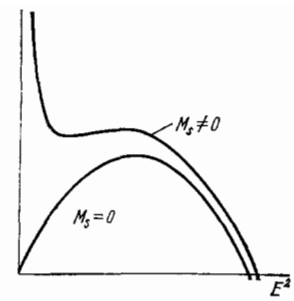

FIG. 14. Effective rotator energy as a function of the square of the electric field.

$$\varepsilon=1-\frac{ZN}{n_c}-\frac{Z^2N\,|\,\mathbf{E}(x)\,|^2}{16\pi n_c^2M_i(V^2-v_s^2)}.$$

We shall use this to obtain solutions of the Maxwell equations for s-polarized radiation incident on the plasma at an angle θ. In this case, they reduce to the following equation for the complex amplitude $E(x)$:

$$E''(x)+\frac{\omega_0^2}{c^2}\left(\varepsilon_0-\sin^2\theta-\frac{|\,E(x)\,|^2}{E_v^2}\right)E(x)=0, \tag{4.5}$$

where $\varepsilon_0 = 1 - (ZN/n_c)$, $E_v^2 = Z^{-2}N^{-1}16\pi n_c M_i \times (V^2 - v_s^2)$.

Using the formula $E(x) = \mathscr{E}(x)\exp[i\varphi(x)]$, and substituting for the real amplitude $\mathscr{E}(x)$ and phase $\varphi(x)$, we find from (4.5) that

$$\mathscr{E}''-\frac{M^2}{\mathscr{E}^3}+\frac{\omega_0^2}{c^2}\left(\varepsilon_0-\sin^2\theta-\frac{\mathscr{E}^2}{E_v^2}\right)\mathscr{E}=0, \tag{4.6}$$

$$M'=0,$$

where $M = \mathscr{E}^2\varphi'$. Since $M = \text{const}$, we may conclude that (4.6) is equivalent to the equation of motion for the anharmonic rotator. The energy integral for this rotator is

$$(\mathscr{E}')^2+\frac{M^2}{\mathscr{E}^2}+\frac{\omega_0^2}{c^2}\left[(\varepsilon_0-\sin^2\theta)\mathscr{E}^2-\frac{\mathscr{E}^4}{2E_v^2}\right]=\text{const}. \tag{4.7}$$

Figure 14 shows the sum of the centrifugal $(M^2/\mathscr{E}^2)$ and potential $((\omega_0/c)^2[(\varepsilon_0 - \sin^2\theta)\mathscr{E}^2 - (\mathscr{E}^4/2E_v^2)])$ energies of the rotator as a function of the square of the electric field. It follows from this figure that the maximum possible electric field strength in the electromagnetic wave in the ultrasonic plasma flow is bounded[39–41] (see also Refs. 42–44) because regular solutions of (4.6) correspond to states in the interior of the effective potential well of Fig. 14. The two curves in this figure correspond to zero and nonzero values of M. Comparison of these curves will readily show that the propagation of electromagnetic waves in the ultrasonic flow is forbidden above a certain critical electromagnetic-wave energy flux. The following restriction ensues from (4.7):

$$\lambda_0 M\leqslant\left(\frac{2}{3}\right)^{3/2}16\pi\varkappa T\frac{n_c}{ZN}\left(\cos^2\theta-\frac{ZN}{n_c}\right)^{3/2}\left(\frac{V^2}{v_s^2}-1\right). \tag{4.8}$$

For the maximum flux, which corresponds to the equality sign in this formula, the solutionof (4.6) has the form of a plane wave of constant amplitude $E(x) = \sqrt{2/3}E_v \times \sqrt{\varepsilon_0 - \sin^2\theta}\,\exp\left[ix(\omega_0/c)\sqrt{2/3}\right]$. It is clear from Fig. 14 that a reduction in M is accompanied by an increase in the

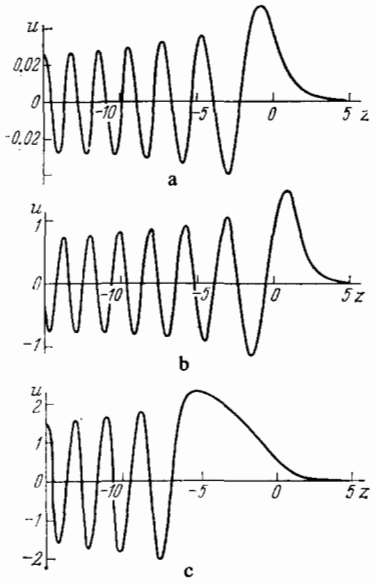

FIG. 15. Electric field in plasma with a linearly inhomogeneous profile as a function of position: a—weak field, b—strong field and subsonic plasma expansion, c—field distribution near the maximum field allowed by the Painlevé equation.

maximum possible electric field, the highest value of which is given by

$$E_{max} = E_v \sqrt{\varepsilon_0 - \sin^2\theta} \tag{4.9}$$

for $M = 0$. Let us elucidate the essence of the field self-limitation effect in ultrasonic plasma flows that we have established. The point is that, because of the raking up of the plasma into the strong-field region, the increase in plasma density makes the plasma less transparent, which impedes the establishment of the field in this plasma and leads to a limitation on the absolute field strength.

We must now reproduce one further result from Ref. 39. This refers to the case of a given (linear) plasma density profile $n = n_c(x + L)/L$ and normally incident radiation. In our case of defocusing nonlinearity, we then have

$$E'' - \frac{\omega_0^2}{c^2}\left[\frac{x}{L} + \left(\frac{E}{E_v}\right)^2\right] E = 0. \tag{4.10}$$

As we enter the opacity region, the field decreases and assumes the form corresponding to the asymptotic linear equation obtained from (4.10) by neglecting the term proportional to E^3. This asymptotic behavior is described by the asymptotic form of the Airy function

$$E(x) = \frac{\mathfrak{A}}{2\sqrt{\pi}} E_v \left(\frac{\lambda_0}{L}\right)^{1/3} \left(\frac{\lambda_0^2 L}{x^3}\right)^{1/2} \exp\left\{-\frac{2}{3}\left(\frac{x^3}{\lambda_0^2 L}\right)^{1/2}\right\}. \tag{4.11}$$

For small values of the constant $\mathfrak{A}$, the solutions obtained by numerical integration of (4.10) are practically indistinguishable from the Airy function. This is clear from Fig. 15a which shows the solution of (4.10) with the asymptotic form (4.11) for $\mathfrak{A} = 0.1$. The situation changes as $\mathfrak{A}$ increases. In particular, because of the deformation of the density distribution, the field maximum shifts toward the more rarefied plasma layers, which can be seen in Fig. 15c, plotted for $\mathfrak{A} = 1.4169$. However, the most essential point is that there is no finite solution of (4.10) when the asymptotic form is given by (4.11) and $\mathfrak{A} > \sqrt{2}$. This fact was established in the theory of the Painlevé equation of the second kind.[45] This absence of solutions of the field equation (4.10) corresponds to the field self-limitation effect in spatially inhomogeneous plasma. To demonstrate the qualitative difference between fields in ultrasonic and subsonic flows, Fig. 15b shows, for a focusing nonlinearity ($E_v^2 < 0$) with $\mathfrak{A} = 10$, how the field shifts into the interior of the plasma rather than in the outward direction, as was the case in Fig. 15c for ultrasonic flow.

Our analytic results enable us to conclude that, when there is little dissipation of electromagnetic field energy, and the scale of the spatial change in density in an inhomogeneous ultrasonic plasma flow is not too small, the electric field strength in the radiation incident on the plasma exhibits the self-limitation effect and oscillates in space, i.e., it does not increase as in linear electrodynamics or the nonlinear electrodynamics of subsonic flows. On the contrary, as it enters the plasma, and before it reaches the opaque layer, the field amplitude shows a decreasing oscillating behavior. This conclusion is confirmed by Fig. 16, which compares the penetration of weak (linear theory) and strong (b) fields into the one-dimensional ultrasonic flow of an expanding plasma. This picture was obtained[40] by solving the equations of Sec. 3 for the field of s-polarized radiation.

Definite experimental confirmation of the field self-limitation effect in ultrasonic flows was reported in Refs. 40 and 41, where a study was carried out of the temporal evolution of the interaction between neodymium laser radiation and aluminum plasma. It was found that second-harmonic generation (Fig. 17a) and weak back-reflection of incident radiation (Fig. 17b) were time-correlated with the first half of the pulse, when the reflected spectrum was shifted to the red. Conversely, second-harmonic radiation and absorption of

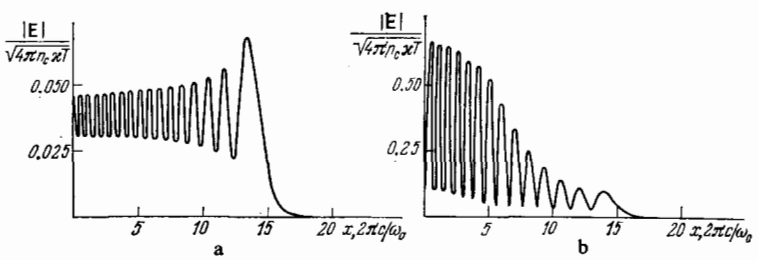

FIG. 16. Field penetration into an ultrasonically expanding plasma: a—weak field, b—strong field.

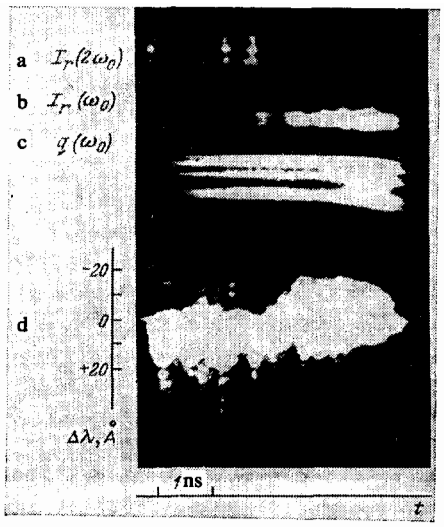

FIG. 17. Experimental time dependence of : second harmonic generation (a), backward reflection of laser radiation (b), intensity of laser radiation (c), and spectral composition of back-reflected radiation (d).

radiation were substantially suppressed in the second half of the pulse heating the laser plasma, which was characterized by a considerable blue shift of back-reflected radiation, indicating the ultrasonic character of the flow. This may be regarded as an indication of a considerable reduction in the electromagnetic field penetrating the critical-density region, in accordance with the field self-limitation effect due to the ponderomotive force that arises in ultrasonic flow and rakes up the plasma into the strong-field region, which means that the existence of the wave field in plasma is forbidden.

5. PARAMETRIC TURBULENCE AND THE ASSOCIATED ABSORPTION OF RADIATION

Among the possible nonlinear phenomena that occur in plasma illuminated by powerful electromagnetic radiation, there is considerable interest in the wide class of parametric effects.[27] In physical descriptions of the anomalous interaction between powerful laser radiation and plasma, it is then important rigorously to take into account the spatial inhomogeneity of the real laser plasma, which is seen as a change in the parametric instability thresholds and the spatial localization of parametric turbulence. The latter fact is reflected in the suppression of parametric turbulence of laser plasma as compared with the hypothetical spatially-homogeneous model. Moreover, we emphasize that it has been shown[46] (see also Refs. 47 and 48) that overestimates of this suppression led in the past to a substantial underestimate of the rate of anomalous absorption of laser radiation.

To illustrate the ideas of the theory of parametric turbulence in spatially inhomogeneous plasmas, we shall suppose that the electron (and ion) density is a linear function of a single coordinate:

$$n(x) = n_0\left(\text{const} + \frac{x}{L}\right), \tag{5.1}$$

where L is the characteristic linear dimension of the inhomogeneity. We shall examine certain consequences of the theory of parametric instabilities in the neighborhood of regions in which the electron density is equal to the critical value (n_c) or one-quarter of the critical value ($n_c/4$).

We begin with the theory of decay of the pump wave into two plasmons, $t \to 2l$, which occurs near $n_c/4$.

This instability was investigated in Refs. 49 and 50 within the framework of the theory of homogeneous plasmas. The role of plasma inhomogeneity in the development of this instability was investigated in Refs. 51–54. Here, we must note the absolute parametric instability of the decay of the pump wave into two plasmons, established in these papers. It has been shown[51,54,55] that the size of the region of spatial localization of growing plasma perturbations with a given wave vector component at right angles to the direction of the spatial inhomogeneity is determined by the relatively small quantity

$$\sim \frac{v_E}{c} L, \tag{5.2}$$

where c is the velocity of light and $v_E = |e|E_0/m_e\omega_0$ is the amplitude of the electron velocity oscillations in the pump-wave electric field

$$E(x, t) = E_0 \sin(\omega_0 t - \int k_0\, dx).$$

The fact that the quantity given by (5.2) was small has led to the conclusion[56] that the anomalous absorption of laser radiation at one-quarter of the critical density was small. This conclusion resulted from an analysis of solitons produced parametrically in this region. However, Erokhin and Silin[46] have shown that this conclusion was merely a consequence of artificial self-limitation resulting from the use of only one-dimensional solitons. On the contrary, multidimensional soliton solutions can fill a very wide region, determined by the linear theory of parametric two-plasmon decay and corresponding to the set of regions (5.2) containing plasmons with different transverse wave-vector components.[54,48] Provided we are then not too near to the threshold, the total linear size of the region in which parametric instability develops is

$$\Delta x \sim 3Lr_{De}^2 k_{max}^2, \tag{5.3}$$

where r_{De} is the electron Debye length and k_{max} is the maximum permissible magnitude of the plasmon wave vector. This result is a consequence of elementary (but unnoticed in soliton theory) ideas on detuning from resonance. Since, in the short-wave region, the limit of instability turns out to be insensitive to the effect of spatial inhomogeneity, the overall size of the two-plasmon decay region turns out to be[54] $\Delta x_{2l} \sim L\,[\ln(c/v_E)]^{-1}$. It is clear that the two-plasmon decay region can occupy a considerable portion of the inhomogeneous profile of the laser plasma corona. We note that Rubenchik's conclusion[57] that the anomalous two-plasmon absorption was small was due to the unjustified assumption that the region of localization of turbulence in two-plasmon decay was small.

The estimated spatial size of the instability region given by (5.3) is very general. Thus, in the case of one further absolute instability, which now occurs near the critical density point, and takes the form of an aperiodic parametric instability[58] that transforms the pump wave into an electron longi-

tudinal Langmuir wave and an aperiodic plasmon perturbation (soliton or caviton), the characteristic size of the region in which this type of instability develops is[48] $\Delta x_{la} \sim L\{\ln[(r_{De}^2 + r_{Di}^2)/r_E^2]\}^{-1}$, where r_{Di} is the ion Debye length and $r_E = v_E/\omega_0$ is the amplitude of electron oscillations in the pump field. Again, as for two-plasmon decay, the size of the region of parametric instability turns out to be comparable with the size L of the laser plasma corona.

Finally, let us consider the convective decay instability of the transverse pump wave into an electron Langmuir and an ion-acoustic wave.[58,59] Despite the fundamental difference between this instability and the absolute instabilities examined above, the region of convective amplification of a wave with given wave vector is relatively small. Hence, to estimate the size of the entire instability region, we must again use (5.3). For the purposes of estimates, we can take the maximum magnitude of the wave vector to be the value for which Landau damping, which prevents the generation of short-wave plasmons, becomes appreciable. This yields $\Delta x_{ls} \sim L \max\{[\ln(\omega_0/\nu_{ei}]^{-1} 0.3\}$, where ν_{ei} is the electron collision frequency. This formula also shows that the decay instability develops in a region whose size is comparable with the characteristic linear dimension L of plasma inhomogeneity. When the laser radiation energy flux density is not too large, this dimension is determined by the usual hydrodynamics of expanding laser plasma corona. Conversely, when the radiation flux density is high, so that ponderomotive forces steepen the profile of the inhomogeneous plasma density, the quantity L can become relatively small. The above ideas on the localization in space of parametric turbulent regions have now been widely adopted.

Having determined the characteristic dimensions of the region of parametric turbulence, we now turn to the characteristic rate of anomalous absorption of radiation, typical for such turbulence. We shall base this on the concept of effective collision frequency ν_{eff} that is a measure of the rate of transformation of the electromagnetic pump energy $E_0^2/4\pi$ into plasma waves and heat. The power transformed in this way is given by

$$Q = \nu_{eff} \frac{E_0^2}{4\pi}. \tag{5.4}$$

To determine Q and hence ν_{eff}, we must consider the excitation of electron Langmuir waves with wave vector k_d and the corresponding parametric instability growth rate $\gamma \equiv \gamma(E_0, k_d)$. We shall propose that k_d is not too small, i.e., $k_d r_{De} > \omega_{Li}/\omega_{Le}$, so that the dispersion correction to the Langmuir-wave frequency is greater than the ion-acoustic frequency of nonisothermal plasma. Secondary parametric instability against the excitation of Langmuir (and low-frequency) plasma waves is then the main process of nonlinear wave interaction in a relatively wide range of parameter values. If we let γ_k represent the growth rate of this instability, the power pumped into the plasma is given by

$$Q = \gamma_k \frac{E_{l\gamma}^2}{4\pi}, \tag{5.5}$$

where $E_{1\gamma}$ is the field in the electron Langmuir oscillations in the pumped region. Since γ_k is a function of E_1, we can determine $E_{1\gamma}$ by assuming quasistationarity in the pumped region, i.e., if we equate the growth rates of primary (γ) and secondary γ_k parametric instabilities at $k = k_d$:

$$\gamma_{k=k_d}(E_{l\gamma}) = \gamma(E_0 k_d). \tag{5.6}$$

We can now use (5.6) to determine the transformed radiation power[60] for different secondary parametric processes. First, for nonisothermal plasma and weak coupling between the parametrically excited waves, i.e., for

$$\gamma < \omega_{Li} k_d r_{De}, \tag{5.7}$$

so that the electron Langmuir wave decays into another such wave and sound, the instability growth rate is

$$\gamma_{k_d} = (\omega_{Le}\omega_{Li} k_d r_{De})^{1/2} E_{l\gamma} (32\pi n_e \varkappa T_e)^{-1/2}. \tag{5.8}$$

According to (5.6), we then have the following expression[61] for (5.5):

$$Q \cong \frac{8 n_e \varkappa T_e \gamma^2}{\omega_{Le}\omega_{Li} k_d r_{De}}. \tag{5.9}$$

In isothermal plasma, the decay rate of ion-acoustic waves is comparable with the frequency of sound, i.e., $\gamma_s \sim \omega_{Li} r_{De} k_d$, so that, if (5.9) is valid, the secondary-instability growth rate is

$$\gamma_k \approx \omega_{Le} \frac{E_{l\gamma}^2}{32\pi n_e \varkappa T_e}. \tag{5.10}$$

Taken together with (5.6), this expression gives the following expression for the energy pumped into the plasma:

$$Q \approx 8 n_e \varkappa T_e \frac{\gamma^2}{\omega_{Le}}, \tag{5.11}$$

which was obtained in Ref. 62.

Let us now determine ν_{eff} under the conditions of weak coupling (5.10). For primary parametric instability corresponding to the $t \to l + s$ decay, for which the growth rate is given by a formula such as (5.11), we find that[84]

$$\nu_{eff}^{(ls)} \sim 2\gamma \lesssim \omega_s. \tag{5.12}$$

For primary parametric instability in isothermal plasma that corresponds to the aperiodic process $t \to l + a$ for which the growth rate is given by a formula such as (5.10), we find from (5.11) that

$$\nu_{eff}^{(la)} \sim \frac{\omega_0^2}{\omega_s} \frac{v_E^4}{v_{Te}^4} \lesssim \omega_s. \tag{5.13}$$

Finally, for primary parametric instability corresponding to the two-plasmon decay $t \to 2l$ with the rate

$$\gamma_{2l} \sim \omega_{Le} \frac{v_E}{c}. \tag{5.14}$$

we find that, in nonisothermal plasma for which (5.9) holds, we have[61]

$$\nu_{eff}^{(2l)} \sim \omega_0 \frac{v_{Te}^2}{c^2} \frac{\omega_{Le} v_E}{\omega_{Li} r_{De} k_d c} \lesssim \omega_0 \frac{v_{Te}^2}{c^2}. \tag{5.15}$$

For isothermal plasma, we find with the aid of (5.11) that

$$\nu_{eff}^{(2l)} \sim \omega_0 \frac{v_{Te}^2}{c^2}. \tag{5.16}$$

A similar formula was obtained in Ref. 57. Equations (5.12), (5.13), and (5.15), (5.16) readily allow values exceeding the electron-ion collision frequency, and hence correspond to very effective transformation of electromagnetic energy into

longitudinal electron Langmuir waves. Under the conditions of weak coupling, such waves can then be absorbed as a result of electron-ion collisions. The higher rate of absorption actually corresponds to a strong plasma field that arises in the plasma as a result of parametric transformation.

We now turn to pump fields that are strong enough for (5.7) to be violated, so that one can speak of strong parametric-wave coupling. The spectrum of low-frequency oscillations is then essentially determined by the field:

$$\omega_k \sim \gamma_k \sim (\omega_{Le}\omega_{Li}^2 k_d^2 r_{De}^2)^{1/3} \left(\frac{E_{l\gamma}^2}{4\pi n_e \varkappa T_e}\right)^{1/3} \sim E_{l\gamma}^{2/3}. \quad (5.17)$$

At the same time, if both (5.7) is violated and the growth rate is small in comparison with the dispersive correction to Langmuir wave frequency

$$\omega_s = \omega_{Li} r_{De} k_d < \gamma < \omega_{Le} (k_d r_{De})^2, \quad (5.18)$$

the spectral transformation preserves the decay character in the pumped region, but with a modified low frequency. An aperiodic instability is then found to arise for sufficiently long wavelength secondary products with $k_a < k_d$, for which $\gamma_{k_a} = \omega_{Le}(k_a r_{De})^2$. However, the balance condition (5.6) is important for our purposes, and is determined by the secondary decay process under the conditions of (5.10). Since for (5.18) the secondary parametric process is determined by the growth rate (5.17), equation (5.6) yields[60]

$$Q = \frac{\gamma^4 n_e \varkappa T_e}{\omega_{Le}\omega_{Li}^2 k_d^2 r_{De}^2}.$$

Finally, for high growth rates, for which $\gamma > \omega_{Le} k_d^2 r_{De}^2$, the aperiodic instability occurs directly in the pumped region, and is therefore a secondary process that determines the balance with the pumped-in energy through parametric instability. The aperiodic instability growth rate is then $\gamma_k \sim \omega_{Li} E_{l\gamma}(4\pi n_e \varkappa T_e)^{-1/2}$, and if we substitute this in (5.6), and use the expression $E_{l\gamma} = [\gamma(E_0, k_d)/\omega_{Li}](4\pi n_e \varkappa T_e)^{1/2}$ in (5.5), we obtain[63]

$$Q = \frac{\gamma^3}{\omega_{Li}^2} n_e \varkappa T_e.$$

The power that is parametrically transformed into longitudinal waves in the absence of secondary aperiodic instability is absorbed as a result of electron-ion collisions. Conversely, for long wavelength waves, for which $k < k_a$, aperiodic instability can shift the Langmuir instability along the spectrum into the short-wave region and give rise to Cherenkov absorption by electrons, which may be an effective mechanism for the generation of hot electrons.

We note in conclusion that inclusion of convection in the description of convective instabilities such as the $t \to l + s$ decay under the conditions of spatially-inhomogeneous plasmas, rather than of the balance of (5.6), requires that the spatial increments in the growth rates of primary and secondary parametric instabilities must be equal.[64,65] The effective collision frequency is then $\nu_{eff} \sim 0.1 k_d v_E$, which may exceed the value given by (5.12).

6. ABSORPTION OF RADIATION DUE TO ION-ACOUSTIC TURBULENCE

The absorption of powerful electromagnetic radiation by plasma is accompanied by the appearance of a heat flux transported by plasma electrons. This heat flux may be the cause of ion-acoustic instability[66] that produces ion-acoustic turbulence. The presence of high-intensity ion-acoustic fluctuations can be the cause of additional absorption of electromagnetic radiation when, for example, electromagnetic waves are transformed by ion sound into longitudinal-field pertubations that can be absorbed via the scattering of electrons oscillating in the wave field and the Cherenkov process on electrons. The question of absorption of radiation by tranformation on ion fluctuations into longitudinal perturbations was examined some time ago[67] together with the implications for laser plasmas.[68] The authors of Refs. 69–72 have used a qualitative approach to the analysis of ion-acoustic absorption, and showed that this absorption can be strong when the level of ion-acoustic turbulence is high enough. Here we must emphasize that previous studies were carried out under the conditions of theoretically unproved distributions of ion-acoustic turbulence. It is interesting in this connection to consider recent results of the theory of ion-acoustic turbulence,[73–76] based on the model that takes into account stimulated scattering of ion sound by ions, and quasilinear scattering of electrons by ion sound. This model preserves the Kadomtsev-Petviashvili law for the distribution of turbulent pulsations over the magnitude of the wave vector. It has led to an analytic law for the angular distribution of such pulsations, and has removed the qualitative disagreement with the Kadomtsev-Petviashvili model which overestimates the turbulent-pulsation intensity.

According to Ref. 74, ion-acoustic turbulence originates from the vector expression $\mathbf{R} = n_e e\mathbf{E} - \nabla(n_e \varkappa T_e)$, i.e., the sum of the quasistationary electron field and the density and temperature gradients. In particular, when the main mass of electrons is described by the Maxwellian distribution, the turbulent pulsations are described by $N(k, \cos\theta) = N(k)\Phi(\cos\theta_k)$ where $N(k)$ is the Kadomtsev-Petviashvili distribution, while the angular distribution $[\Phi(\cos\theta_k)]$ and the fluctuation intensity itself depend on the Knudsen number

$$K_N = \frac{3\pi r_{Di}^2 R}{r_{De}^2 m_e n_e v_s \omega_{Li}}. \quad (6.1)$$

the angular distribution for $K_N \gg 1$ is illustrated[76] in Fig. 18 (curve 1) which also gives for comparison the result of a numerical simulation[77] (curve 2).

In accordance with Ref. 67, ion-acoustic absorption of electromagnetic radiation of frequency ω_0, wave vector $\mathbf{k}_0$, and polarization $\mathbf{e}_0$ can be characterized by the following effective collision frequency:[78]

$$\nu_{eff}^{(l)} = \int \frac{d\mathbf{k}}{(2\pi)^3} \frac{\omega_{Le}^2 \omega_s(k) N(\mathbf{k})(\mathbf{k}\mathbf{e}_0)^2}{\omega_0 n_e \varkappa T_e k^2} \frac{\mathrm{Im}\,\varepsilon_l(\omega, k)}{|\varepsilon_l(\omega, k)^2|}, \quad (6.2)$$

where ε_l is the longitudinal permittivity and it is assumed that $k \gg k_0$ and $\omega_0 \gg \nu_{eff}^{(l)}$.

For the axially-symmetric distributions of Refs. 69-72, the formula given by (6.2) can be written in the form $\nu_{eff}^{(l)} = e_{0x}^2 \nu_{\parallel}^{(l)} + (e_{0y}^2 + e_{0z}^2)\nu_{\perp}^{(l)}$ where the x axis lies along the vector $\mathbf{R}$, $\nu_{\perp}^{(l)} = (1/2)(M_0 - M_1)\bar{\nu}$, $\nu_{\parallel}^{(l)} = M_1 \bar{\nu}$, and

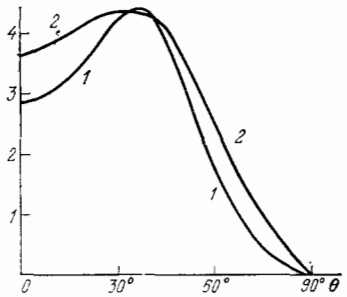

FIG. 18. Angular distribution of ion-acoustic turbulence for high turbulent Knudsen numbers: 1—analytic theory, 2—result obtained by the particle method.[77]

$$M_n = \int_0^1 \mathrm{d}\,(\cos\theta)\cos^{2n}\theta\Phi(\cos\theta), \quad \tilde{\nu} = \frac{1}{4}\frac{v_s^2}{v_{Ti}^2}\omega_{Li}N(\omega_0),$$

$$N(\omega_0) = \sqrt{\frac{2}{\pi}}\frac{\omega_{Le}}{\omega_0} \times \int_{r_{De}k_{min}}^{1} \mathrm{d}x\, x^{-4}\ln x^{-1}\,\mathrm{Im}\,\varepsilon_l(\omega_0,\ xr_{De}^{-1})\,|\varepsilon_l(\omega_0,\ xr_{De}^{-1})|^{-2}.$$

In the limit as $\omega_0^2 \ll 2\omega_{Le}^2$ we have $N(\omega_0) \approx 1$. This limit corresponds to the physical picture of dissipation found in Ref. 79 and involving energy loss by an electron oscillating in the radiation field when it is scattered by ion-acoustic fluctuations.

We shall now follow Ref. 79 and examine the dependence on the turbulent Knudsen number and the anisotropy of effective collision frequencies. In the limit as $K_N \gg 1$, we have[76] $M_n = m_n\sqrt{K_N}$, where $m_0 = 2.04$ and $m_1 = 1.10$. Consequently, the anisotropy is small in this limit, and the effective collision frequencies are $\sim\sqrt{K_N}$. In the opposite limit $K_N \ll 1$, and provided we are not too close to the threshold for ion-acoustic instability ($K_{st} \gg 1$), we can use the angular distributions taken from Refs. 69–72 to obtain

$$M_n = \frac{4K_N}{3\pi}\int_0^1 \mathrm{d}\xi\,\xi^{2n-1}\frac{d}{d\xi}\frac{\xi^4}{1+\Delta-\xi},$$

where $\Delta = \max(\delta; (8K_N/3\pi)\ln K_N^{-1})$ and $\delta = (\omega_{Le}/\omega_{Li}) \times (ZT_e/T_i)^{3/2}\exp(-ZT_e/T_i)$. In the limit of a small departure from the isothermal state, $\delta \gg 1$, we have $\nu_\perp^{(l)} = (1/3)\nu_\parallel^{(l)}$ and $M_1 = (16/15\pi)(K_N/\delta)$. In the opposite case of a highly nonisothermal plasma, for which $\delta \ll 1$, the anisotropy of the effective collision frequencies becomes particularly great ($\nu_\parallel^{(l)} \gg \nu_\perp^{(l)}$). Actually, for $\Delta \ll 1$ we have $M_1 = 4K_N/3\pi\Delta$, $M_0 - M_1 = (8K_N/3\pi)$ in Δ^{-1}. Hence it follows that, for $\delta \gg (8K_N/3\pi)\ln K_N^{-1}$, the effective collision frequencies are proportional to K_N. If, on the other hand, $1 \gg (8K_N/3\pi)\ln K_N^{-1} \gg \delta$, the low effective collision frequency $\nu_\perp^{(l)}$ increases with increasing K_N whereas $\nu_\parallel^{(l)}$ varies slowly since, in this limit, $M_1 = (1/2)[\ln K_N^{-1}]^{-1}$. We emphasize that the well-defined anisotropy of the effective collision frequencies that corresponds to this limit ensures that p-polarized radiation is more readily absorbed. The optical thickness of plasma that corresponds to the absorption of p-polarized radiation in this limit is then given by

$$\tau^{(l)} = \sin^2\theta\,\frac{L\omega_{Li}v_s^2}{8cv_{Ti}^2}\overline{N(\omega_0, x)\left(\ln\frac{1}{K_N}\right)^{-1}}, \qquad (6.3)$$

where the average is evaluated over the inhomogeneous plasma layer in which the radiation originates. Since in a sufficiently tenuous plasma $\omega_{Le}^2(x) < (1/2)\omega_0^2$, the effective collision frequency is found to decrease as $\sim\exp[-\omega_0^2/2\omega_{Le}^2(x)]$, and (6.3) corresponds to substantial absorption of radiation incident on plasma at angles[74] $\lesssim 60°$. It is clear that the absorption maximum in (6.3) as a function of the angle of incidence will in general depend on the form of the plasma density distribution.

We note in conclusion that, as shown in Refs. 78 and 74, apart from ion-acoustic absorption, a high level of turbulent pulsations can lead to considerable Mandel'shtam-Brillouin scattering. This scattering may ensure that the fraction of scattered radiation becomes comparable with the fraction absorbed by ion-acoustic pulsations if the turbulence spec-

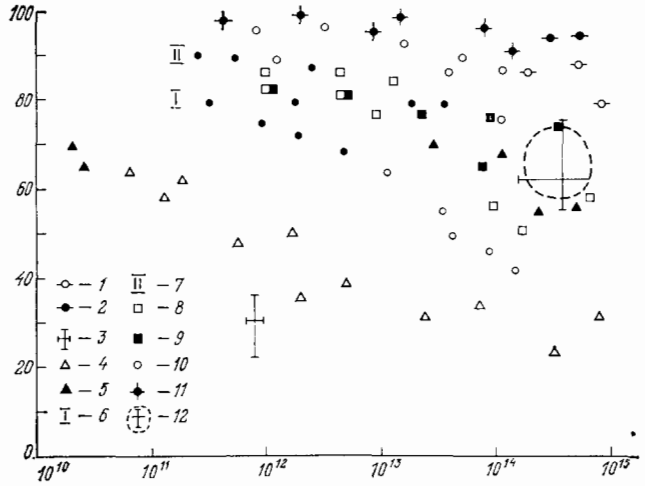

FIG. 19. Experimental data on the absorption coefficient A as a function of laser flux density q (W/m^2) under different conditions: 1—1.06 μm, 2—0.53 μm, 30 ps, copper target (garching), 3—10 μm, 1.5 ns, 4—1.06 μm, 100 ps, 5—0.52 μm, 80 ps, 6—0.53 μm, 2 ns, polyethylene target (Palaiseau), 7—1.06 μm, 2.5 ns, 8—1.06 μm, CH_2, 9—1.06 μm, Au, 10—0.53 μm, CH_2, 500 ps, 45°, 11—0.53 μm, 100 ps, 23°, 12—10 μm, 1 ns (Osaka).

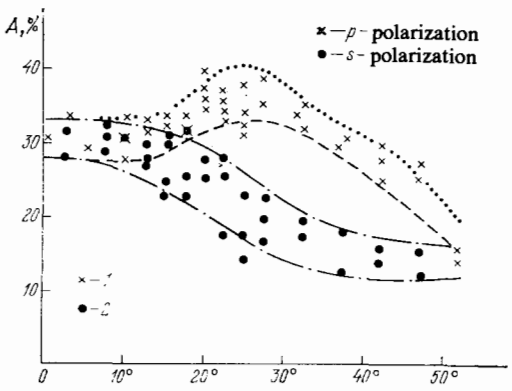

FIG. 20. Angular dependence of absorption A of p-polarized (1) and s-polarized (2) radiation.

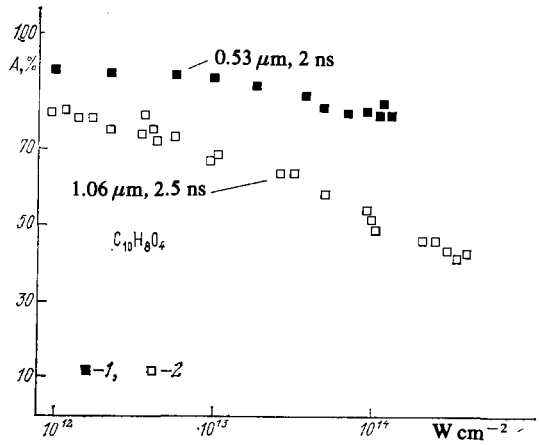

FIG. 21. Absorption by $C_{10}H_8O_4$ plasma.

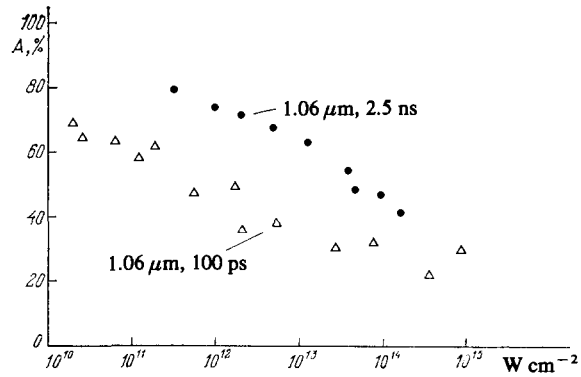

FIG. 22. Absorption of neodymium laser radiation by $C_{10}H_8O_4$ plasma for two pulse lengths—100 ps and 2.5 ns.

trum contains sufficiently long waves ($k_{\min} \lesssim \omega_0/c$). In the model that we have used, this condition is satisfied for[74] $\nu_{ii}\omega_{Le}/\omega_{Li}^2 \lesssim (v_{Te}/c)r_{De}^2/r_{Di}^2$, which is readily satisfied in modern laser-plasma experiments. At the same time, we emphasize that this result may become modified when the turbulence model is improved by taking into account the width of the resonances (see, for example, Ref. 80).

CONCLUSION

The very formulation of the laser fusion problem demands that a substantial fraction of the incident energy must enter the plasma. The fact that the usual collisional absorption decreases rapidly with both plasma temperature and field strength has for long drawn the attention of researchers to the necessity for studying anomalous absorption processes. Many such processes are now helping us to understand experimentally established relationships. At the same time, the conditions under which collisional absorption plays a dominant role have now been identified.

Figure 19 shows a summary[43] of experimental data on laser absorption obtained in the course of the last few years in experiments with planar targets in different laboratories around the world.

The relatively strong absorption of short-wave laser radiation is related to the importance of electron-ion collisions [see Eq. (1.7)]. Conversely, the absorption of CO_2-laser radiation is usually interpreted in terms of resonant absorption on a plasma profile steepened by a strong enough ponderomotive force.

Crude data on total absorption over a relatively wide range are consistent with the theory of collisional and resonant absorption. Further hypotheses are however necessary to explain the more detailed data. For example, Fig. 20 (taken from Ref. 81) demonstrates the difference between the absorption of s- and p-polarized CO_2-laser radiation. Attempts to explain these data in terms of resonant absorption lead to the estimated figure of 10–20 μm for the scale of the spatial variation in the plasma-density profile. This characteristic scale and the temperature $T_e = 0.23$ keV have led the authors of Ref. 81 to the result $A < 5\%$ for the estimated collisional absorption. The much stronger absorption illustrated in Fig. 20 at $\theta = 0°$ for the long focal length of the lens used in Ref. 81, and the associated small divergence of the beam $\Delta\theta \sim 3°$, may be due to (according to the authors of Ref. 81) the transverse corrugation of the plasma density ($L_{tr} \sim (\lambda_0)$, or the strong magnetic field (about 10^6 G), or some other results of the strong interaction between incident radiation and plasma.

In the above review we have ignored the effects of plasma heating by very powerful laser radiation, for which there is a considerable increase in the role of stimulated Raman scattering (see, for example, Ref. 82). Parametric instability may also be important under these conditions. We note in this connection the paper by Kindel[83] which reports an increase from 20 to 70% in the rate of absorption of CO_2-laser radiation when the radiation flux density is increased from 10^{14} to 10^{15} W/cm^2. At the same time, it was suggested that, for the latter flux density, absorption was governed by the following processes: resonant absorption by linear inhomogeneity—20%, resonant absorption by corrugation (assumed absent at lower laser flux densities)—30%, absorption by stimulated Raman scattering—20%. We note that the data on CO_2-laser absorption also indicate an increase in absorption with increasing radiation flux density.

To exhibit more clearly the experimental relationships, Fig. 21 shows the results reported by the Ecole Polytechnique (France) on the absorption of radiation by a flat $C_{10}H_8O_4$ target illuminated by first-harmonic neodymium laser radiation (1; 1.06 μm, pulse length 2.5 ns) and also by second-harmonic radiation (2; 0.53 μm, 2 ns). The increase in absorption with decreasing wavelength is a manifestation of collisional (inverse bremsstrahlung) absorption. The reduction in wavelength corresponds to an increase in the critical plasma density and, secondly, an increase in electron density leads to a reduction in electron temperature for a comparable fraction of absorbed energy. Both phenomena lead to an increase in the effective collision frequency and in the optical thickness due to electron-ion collisions.

Another experimental relationship is illustrated in Fig. 22 which compares data on the absorption of neodymium laser radiation by a flat $C_{10}H_8O_4$ target for two pulse lengths (1; 100 ns and 2; 2.5 ns). It is clear from this figure that absorption increases with increasing laser pulse length. This

increase is due to the increase in the inhomogeneity scale of the expanding plasma which, on the one hand, leads to reduced absorption due to the transformation of laser radiation into the longitudinal plasma field and, on the other hand, to an increase in inverse bremsstrahlung absorption. The importance of the latter effect[85] is indicated by the data of Fig. 22.

The relative importance of different processes in the absorption of laser radiation by plasma can be established only on the basis of factual information on the internal state of the plasma which, undoubtedly, is much simpler to obtain in large-scale laboratory experiments than in laser plasma. There is no doubt that numerical programs capable of dealing with the global behavior of expanding plasmas will continue to play an important role. The formulation of these programs relies on the availability of a realistic theory of the transfer of energy absorbed by the plasma. The development of this theory requires a modification of the methods used to determine the radiation flux when the mean free path is comparable with the characteristic scale of the inhomogeneity, as well as the elucidation of the possible role of magnetic fields generated in laser plasma and an understanding of the role of turbulent processes. In view of this, studies of the absorption of laser radiation by plasmas are nowadays based on experimental data, the exhaustive analysis of which demands a deep understanding of transport processes that have not as yet been fully investigated. However, such processes will have to be reviewed separately.

[1]V. P. Silin, Vvedenie v kineticheskuyu teoriyu gazov (Introduction to the Kinetic Theory of Gases), Nauka, Moscow, 1971.
[2]V. L. Ginzburg, Rastprostranenie elektromagnitnykh voln v plazme , Nauka, Moscow, 1967. [Engl. Transl., The Propagation of Electromagnetic Waves in Plasmas, 2nd ed., Pergamon Press, Oxford, 1970].
[3]N. G. Denisov, Zh. Eksp. Teor. Fiz. **31**, 609 (1956) [Sov. Phys. JETP **19**, 544 (1957).
[4]V. B. Gil'denburg, Zh. Eksp. Teor. Fiz. **45**, 1978 (1963) [Sov. Phys. JETP **18**, 1359 (1964)].
[5]A. D. Piliya, Zh. Tekh. Fiz. **36**, 818 (1966) [Sov. Phys. Tech. Phys. **11**, 609 (1966)].
[6]A. Ya. Omel'chenko and K. N. Stepanov, Ukr. Fiz. Zh. **12**, 1445 (1967); A. Ya. Omel'chenko *et al.*, Izv. Vyssh. Uchebn. Zaved. Radiofiz. **14**, 1484 (1971).
[7]K. G. Budden, Radio Waves in the Ionosphere, Cambridge University Press, 1961, p. 351.
[8]D. L. Kelley and A. Banos, Jr., UCLA Plasma Physics Group Report No. PPG-170, 1974.
[9]D. W. Forslund, J. M. Kindel, K. Lee, E. L. Lindman, and R. L. Morse, Phys. Rev. A **11**, 679 (1976).
[10]T. Speziale and P. J. Catto, Phys. Fluids **20**, 990 (1977).
[11]G. J. Pert, Plasma Phys. **20**, 175 (1978).
[12]F. David, Rapport d'Activité 1979 du GRECO ILM, Palaiseau Cedex, Ecole Polytechnique, 1979.
[13]W. Woo, K. Estabrook, and J. S. De Groot, Phys. Rev. Lett. **40**, 1094 (1978).
[14]A. Montes and M. Hubbard, Plasma Phys. **21**, 885 (1979).
[15]Yu. Aliev, O. M. Gradov, and A. Yu. Kyrie, Phys. Rev. **15**, 2120 (1977); Yu. M. Aliev, S. Vukovich, O. M. Gradov, A. Yu. Kiriĭ, and V. Chadezh, Pis'ma Zh. Eksp. Teor. Fiz. **25**, 351 (1977) [JETP Lett. **25**, 326 (1977)].
[16]A. A. Zharkov, I. G. Kondrat'ev, and M. M. Miller, Pis'ma Zh. Eksp. Teor. Fiz. **25**, 355 (1977) [JETP Lett. **25**, 330 (1977)].
[17]A. G. M. Maaswinkel, Experimental Investigation of Linear Mode Conversion in Laser-produced Plasmas, Projektgruppe für laser forschung, PLF 39, 1980.
[18]V. P. Silin, Zh. Eksp. Teor. Fiz. **47**, 2254 (1964) [Sov. Phys. JETP **20**, 1510 (1965)].
[19]V. P. Silin, Zh. Eksp. Teor. Fiz. **38**, 1771 (1960) [Sov. Phys. JETP **11**, 1277 (1960)].
[20]V. P. Silin, Zh. Eksp. Teor. Fiz. **41**, 861 (1961) [Sov. Phys. JETP **14**, 617 (1962)].
[21]V. P. Silin and S. A. Uryupin, Zh. Eksp. Teor. Fiz. **81**, 910 (1981) [Sov. Phys. JETP **54**,485 (1981)].
[22]Y. Shima and H. Yatom, Phys. Rev. A **12**, 2106 (1975).
[23]R. V. Karapetyan, Thesis for Candidate's Degree, FIAN SSSR, Moscow, 1980.
[24]A. B. Langdon, Phys. Rev. Lett. **44**, 575 (1980).
[25]R. J. Balescu, Plasma Phys. **27**, 553 (1982).
[26]C.E. Max, in: Interaction Laser-plasma, ed. by R. Balian and J.-C. Adam, North-Holland, Amsterdam, New York, Oxford, 1982, p. 316.
[27]V. P. Silin, Parametricheskoe vozdeistvie izlucheniya bol'shoĭ moshchnosti na plazmu (Parametric Interaction of Powerful Laser Radiation with Plasma), Nauka, Moscow, 1973
[28]N. E. Andreev and V. P. Silin, Fiz. Plazmy **4**, 908 (1978). [Sov. J. Plasma Phys. **4**, 508 (1978)].
[29]N. E. Andreev, V. P. Silin, and G. L. Stenchikov, Pis'ma Zh. Eksp. Teor. Fiz. **28**, 533 (1978) [JETP Lett. **28**, 494 (1978)].
[30]N. E. Andreev, V. P. Silin, and G. L. Stenchikov, V kn. Vzaimodeĭstvie sil'nykh elektromagnitnykh voln s besstolknovitel'noĭ plazmoĭ (Interaction of Powerful Electromagntic Waves with Collisionless Plasma), IPF AN SSSR, Gor'kiĭ, 1980, p. 156.
[31]N. E. Andreev, V. P. Silin, and G. L. Stenchikov, Zh. Eksp. Teor. Fiz. **78**, 1396 (1980) [Sov. Phys. JETP **51**, 703 (1980)].
[32]N. E. Andreev, V. P. Silin, and G. L. Stenchikov, Physica D **2**, 146 (1981).
[33]N. E. Andreev, V. P. Silin, and G. L. Stenchikov, Fiz. Plazmy **8**, 600 (1982) [Sov. J. Plasma Phys. **8**, 339 (1982)].
[34]N. E. Andreev, O. M. Gradov, P. Kara, V. P. Silin, and G. L. Stenchikov, Kratk. Soobshch. Fiz. No. 3, 26 (1982).
[35]K. Lee, D. W. Forslund, J. M. Kindell, and E. L. Lindman, Phys. Fluids **20**, 51 (1977).
[36]P. Mulser and C. van Kessel, Phys. Rev. Lett. **38**, 902 (1977).
[37]N. L. Tsintsadze and D. D. Tskhakaya, Zh. Eksp. Teor. Fiz. **72**, 480 (1977) [Sov. Phys. JETP **45**, 252 (1977)].
[38]H. Akiyama, O. Matsumoto, and S. Takeda, in: Proc. Intern. Conf. on Plasma Phys., Nagoya, Japan, 1980, Vol. I, p. 393.
[39]N. E. Andreev, V. P. Silin, and P. V. Silin, Zh. Eksp. Teor. Fiz. **79**, 1293 (1980) [Sov. Phys. JETP **52**, 653 (1980)].
[40]N. E. Andreev, V. L. Artsimovich, Yu. S. Kas'yanov, V. V. Korobkin, V. P. Silin, P. V. Silin, and G. L. Stenchikov, Pis'ma Zh. Eksp. Teor. Fiz. **31**, 636 (1980) [JETP Lett. **31**, 332 (1980)].
[41]N. E. Andreev, V. L. Artsimovich, Yu. S. Kas'yanov, V. V. Korobkin, V.P. Silin, P. V. Silin, and G. L. Stenchikov, Phys. Lett. A **82**, 177 (1981).
[42]V. P. Silin, in: The Physics of Ionized Gases, ed. by M. Matic, Belgrade, 1980, p. 575.
[43]V. P. Silin, in: Proc. Fifteenth Intern. Conf. on Phenomena in Ionized Gases, Invited Papers, Minsk, 1981, p. 357.
[44]N. E. Andreev, V. P. Silin, and P. V. Silin, in: Nonlinear Waves, ed. by L. Debnath, Cambridge University Press, 1983.
[45]M.J. Ablowitz and H. Segur, Phys. Rev. Lett. **38**, 1103 (1977).
[46]A. N. Erokhin and V. P. Silin, Kratk. Soobshch. Fiz. No. 12, 42 (1977).
[47]V. P. Silin, O. poglosheniĭ izlucheniya turbulentnoĭ lazernoĭ plazmoĭ (Absorption of Radiation by Turbulent Laser Plasma), Preprint No. 241, FIAN SSSR, Moscow, 1978.
[48]V. P. Silin, J. Phys. (Paris) Coll. C6, Suppl. No. 12, C6-153 (1977).
[49]J. H. Krenz and G. S. Kino, J. Appl. Phys. **36**, 2387 (1965).
[50]E. A. Jackson, Phys. Rev. **153**, 235 (1967).
[51]V. P. Silin and A. N. Starodub, Zh. Eksp. Teor. Fiz. **66**, 176 (1974) [Sov. Phys. JETP **39**, 82 (1974)].
[52]Y. C. Lee and P. Kaw, Phys. Rev. Lett. **32**, 135 (1974).
[53]C. S. Liu and M. N. Rosenbluth, Phys. Fluids **19**, 976 (1976).
[54]V. P. Silin and A. N. Starodub, Zh. Eksp. Teor. Fiz. **73**, 884 (1977) [Sov. Phys. JETP **46**, 465 (1977)].
[55]V. P. Silin, A. N. Starodub, and M. V. Filippov, Zh. Eksp. Teor. Fiz. **73**, 188 (1977) [Sov. Phys. JETP **46**, 97 (1977)].
[56]H. H. Chen and C. S. Liu, Phys. Rev. Lett. **39**, 881 (1977).
[57]A. M. Rubenchik, in: Proc. Thirteenth Intern. Conf. on Phenomena in Ionized Gases. Contributed Papers, 1977, Part 2, p. 887.
[58]V. P. Silin, Zh. Eksp. Teor. Fiz. **47**, 2254 (1965) [Sov. Phys. JETP **20**, 1510 (1965)].
[59]D. F. Du Bois and M. V. Goldman, Phys. Rev. Lett. **14**, 544 (1965).

[60]V. P. Silin and V. T. Tikhonchuk, Pis'ma Zh. Eksp. Teor. Fiz. **27**, 504 (1978) [JETP Lett. **27**, 474 (1978)].
[61]V. Yu. Bychenkov, V. P. Silin, and V. T. Tikhonchuk, *ibid.* **26**, 309 (1977) [JETP Lett. **26**, 283 (1977)].
[62]W. L. Kruer and E. J. Valco, Phys. Fluids **16**, 675 (1973).
[63]A. A. Galeev, R. Z. Sagdeev, V. D. Shapiro, and V. I. Shevchenko, Zh. Eksp. Teor. Fiz. **73**, 1352 (1977) [Sov. Phys. JETP **46**, 711 (1977)].
[64]V. P. Silin and V. T. Tikhonchuk, Phys. Lett. A **78**, 246 (1980).
[65]V. P. Silin and V. T. Tikhonchuk, Zh. Eksp. Teor. Fiz. **81**, 2039 (1981) [Sov. Phys. JETP **54**, 1075 (1981)].
[66]D. W. Forslund, J. Geophys. Res. **75**, 17 (1970).
[67]J. Dawson and C. Oberman, Phys. Fluids **5**, 517 (1962); **6**, 394 (1963).
[68]J. Fachl and W. L. Kruer, *ibid.* **20**, 55 (1977).
[69]W. M. Manheimer, D. S. Colombant, and B. H. Ripin, Phys. Rev. Lett. **38**, 1135 (1977).
[70]W. M. Manheimer, Phys. Fluids **20**, 265 (1977).
[71]W. M. Manheimer and D. S. Colombant, *ibid.* **21**, 1818 (1978).
[72]D. Colombant and W. M. Manheimer, *ibid.* **23**, 2512 (1980).
[73]V. Yu. Bychenkov and V. P. Silin, in: Proc. Intern. Conf. on Plasma Physics, Göteborg, Sweden, 14 P-11-03, 1982, p. 369.
[74]V. Yu. Bychenkov and V. P. Silin, Zh. Eksp. Teor. Fiz. **82**, 1886 (1982) [Sov. Phys. JETP **55**, 1086 (1982)].
[75]V. Yu. Bychenkov, O. M. Gradov, and V. P. Silin, Zh. Eksp. Teor. Fiz. **83**, 2073 (1982) [Sov. Phys. JETP **56**, 1202 (1982)].
[76]V. Yu. Bychenkov, O. M. Gradov, and V. P. Silin, Fiz. Plazmy **10**, 33 (1984) [Sov. J. Plasma Phys. **10**, 17 (1984)].
[77]D. Biskamp and R. Chodura, Phys. Rev. Lett. **27**, 1553 (1971).
[78]V. Yu. Bychenkov and V. P. Silin, Fiz. Plazmy **9**, 282 (1983) [Sov. J. Plasma Phys. **9**, 165 (1983)].
[79]V. P. Silin, Kratk. Soobshch. Fiz. No. 5, 59 (1983).
[80]W. Horton, Jr. and D. I. Choi, Phys. Rep. **49**, 273 (1979).
[81]C. Garban-Labaune, E. Fabre, F. David, J. Maingnan, and A. Muchard, J. Phys. Lett. **41**, L-463 (1980).
[82]K. Estabrook, W. L. Kruer, and B. F. Lasinski, Phys. Rev. Lett. **45**, 1399 (1980).
[83]J. M. Kindel, The Talk during USA-USSR Workshop on Dense Plasma, Tucson, Arizona, USA, March 7–14, 1983.
[84]W. L. Kruer and E. J. Valeo, Phys. Fluids **18**, 1308 (1973).
[85]Rapport d'Activité du GRECO ILM, Ecole Polytechnique, Palaiseau Cedex, 1982.

Translated by S. Chomet